Computational Design and Prototype Evaluation of Aluminide-Strengthened Ferritic Superalloys for Power-Generating Turbine Applications (up to 1,033K)

P. K. Liaw[1], Z. K. Teng[1], S. Y. Huang[1], C. T. Liu[1], M. E. Fine[2], G. Ghosh[2], M. D. Asta[3], D. Worthington[3], and G. Y. Wang[1]

1. **Department of Materials Science and Engineering, The University of Tennessee, Knoxville, TN 37996, USA**
2. **Department of Materials Science and Engineering, Northwestern University, Evanston, IL 60208-3108, USA**
3. **Department of Chemical Engineering and Materials Science, University of California, Davis, CA 95616, USA**

06-10-2008

Acknowledgements

- The Department of Energy (DOE) Office of Fossil Energy Program, under Grant No. DE-PS26-05NT42472-04.

- Dr. Patricia Rawls, Program Director

Outline

- **Technical Issues**
- **Scientific Basis for Microstructural Design**
- **Objectives**
- **Prototype Evaluation**
    1. Alloy design and fabrication
    2. Microstructure characterization
    3. Ductility measurement
    4. Creep study
- **Initial First-Principles Calculations**
- **Conclusions**

Technical Issues

Ferritic superalloys compare to Ni-based superalloys

Advantages:

- Higher melting temperature
- Superior thermal conductivity
- Lower thermal expansion
- Much less expensive than Ni-based superalloys

Challenges:

- Limited creep resistance at high temperatures
- Brittle at room temperature (RT)

Currently used below 894K, but require increased temperature capability to 1,033K by 2020 [1,2]

[1] C. P. Dogan and I. G. Wright, "Materials for ultra-supercritical steam turbines," paper presented at the 28th International Technical Conference on Coal Utilization & Fuel Systems, Clearwater, FL, March 10-13, 2003.
[2] H. K. D. H. Bhadeshia, "Design of ferritic creep-resistant steels," *ISIJ International*, 41, 626-640 (2001).

Scientific Basis for Microstructural Design

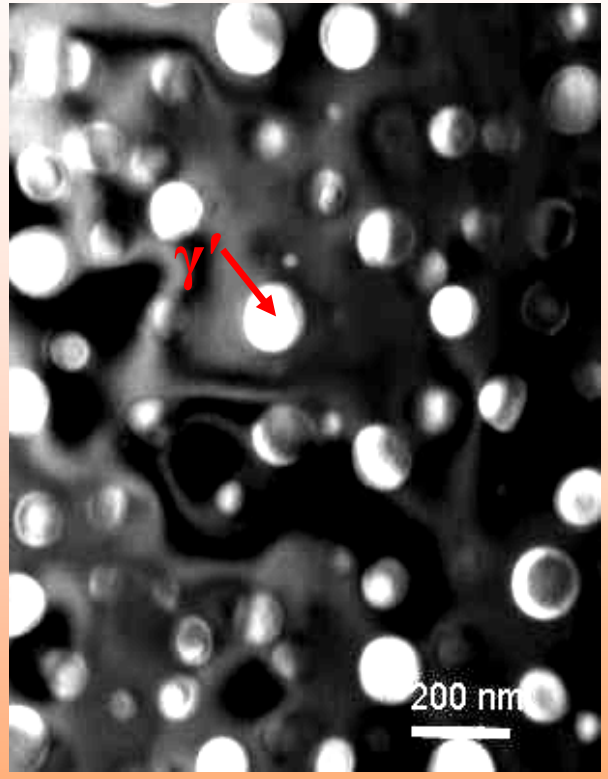

γ/γ′phases in a Ni-based alloy (Ni-22Cr-15Fe) (wt.%) [1]

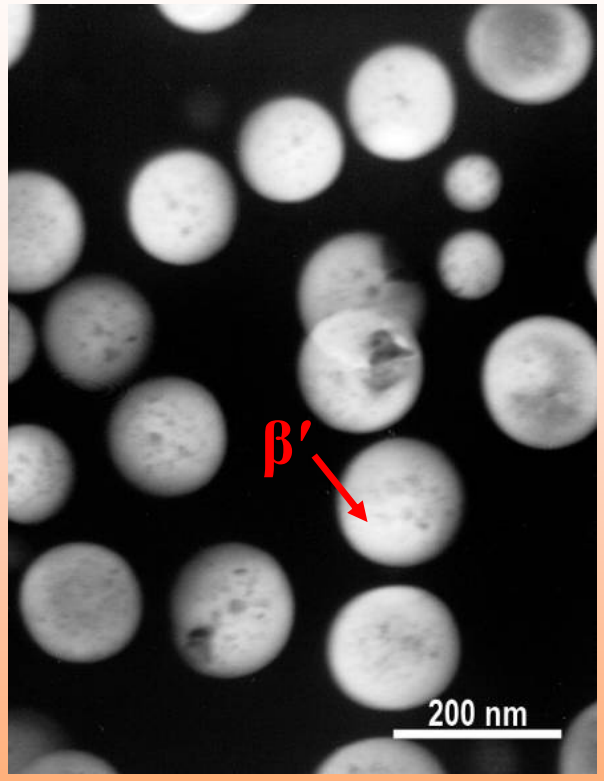

β/ β′ phases in an Fe-based alloy (Fe-6.5Al-10Ni-10Cr-3.4Mo-0.25Zr-0.005B) (wt.%), present work

Nickel-based γ/γ′ superalloys owe their excellent creep strength to the presence of a high volume fraction of coherent-coplanar ordered γ′ precipitates.

Like γ/γ′ systems, the body-centered cubic (bcc) Fe-matrix (A2 or β) and NiAl-type (B2 or β′) precipitates exhibit cube-on-cube or coplanar orientation relationship.

[1] Neal D. Evans, Philip J. Maziasz, and John J. Truhan, “Phase Transformation During Service Aging of Nickel Based Superalloy Pyromet 31V”.

Objectives

- A steady-state creep rate of approximately 3 x 10^{-11} s^{-1} at a temperature of 1,033K and a stress level of 35 MPa.
- Ductility of ~ 10% at RT.
- Good oxidation and corrosion resistance at 1,033K.
- An optimized design requiring slow diffusion in the ferrite matrix for stable microstructures and good creep resistance at elevated temperatures

Systems-Based Materials Design

PROCESSING

- AGING
- HOMOGENIZATION
- FORGING/ROLLING
- SOLIDIFICATION
- DEOXIDATION, REMELTING
- PRIMARY MELTING

STRUCTURE

MATRIX
BCC Solid Solution of Fe
- Lattice Parameter
- Solid-Solution Hardening
- Diffusivity/Mobility (Hf, Ta, W, Zr, Mo)

MICROSEGREGATION
Inhomogeneity

STRENGTHENING DISPERSION
- B2 Based on NiAl and/or
- $L2_1$ Based on Ni_2TiAl
  - Lattice Parameter
  - Misfit Control
- Minimizing Coarsening Rate (Hf, Zr)
- Eliminating TCP phases: Laves, σ, μ

GRAIN-BOUNDARY CHEMISTRY
Sliding Resistance
Precipitates

PROPERTIES

CREEP RESISTANCE
Rafting

TOUGHNESS AND DUCTILITY
(Low Temperature)

OXIDATION/ CORROSION RESISTANCE

PERFORMANCE

COMPUTATIONS
DICTRA, TC
EXPERIMENTS
Arc melting, Hot forging/rolling, SEM

COMPUTATIONS
DFT, ATAT, DICTRA, TC
EXPERIMENTS
HR-AEM, SEM, TEM, XRD

COMPUTATIONS
Creep Modeling
EXPERIMENT
Ambient and Elevated Temperature Mechanical Properties, Oxidation Kinetics

Computational Tools Used and to be Used in the Present Research

- **Electronic Density-Functional Theory (DFT)** code: Vienna Ab Initio Simulation Package (VASP):

  To calculate the total energy and electronic structure of many-body systems.
- **Alloy Theoretic Automated Toolkit (ATAT)**:

  To compute free energies for partially-ordered compounds and solid solutions.
- **Thermo-Calc (TC)**:

  To predict phase stability and phase equilibria as a function of composition and temperature in multi-component alloys.
- **DIffusion Controlled TRAnsformations (DICTRA)**:

  To simulate diffusion-controlled transformations in multi-component systems that involve multiple phases with simple geometries.

Alloy Design and Preparation

Ferritic Beta-Beta Prime (FBB) Alloy
Compositions (in weight percent, wt.%)

Alloy	Fe	Al	Ni	Cr	Mo	Hf	Zr	B	W
FBB-1 (HT1)	70	10	10	10	-	-	-	-	-
FBB-2 (HT1)	66.3	10	10	10	3.4	0.25	-	0.005	-
FBB-3 (HT1)	66.3	10	10	10	3.4	-	0.25	0.005	-
FBB-5 (HT1)	63.2	10	10	10	3.3	-	-	0.005	3.5
FBB-6 (HT1)	65.6	10	10	10	1.7	-	0.25	0.02	2.5
FBB-7 (HT1)	68.3	8	10	10	3.4	-	0.25	0.005	-
FBB-8 (HT1)	69.8	6.5	10	10	3.4	-	0.25	0.005	-
FBB-9 (HT2)	71.3	5	10	10	3.4	-	0.25	0.005	-
FBB-10 (HT2)	71.2	6.5	10	10	2.0	-	0.25	0.005	-
FBB-12 (HT2)	72.3	4	10	10	3.4	-	0.25	0.005	-

Arc melt and drop cast, 12.7 × 12.7 × 76.2 mm

Heat Treatments:

HT1: 1,473 K/30 min. ⟶ 973 K/100 h; HT2: 1,273 K/30 min. ⟶ 973 K/100 h

TEM Examination of FBB-8 (6.5Al)

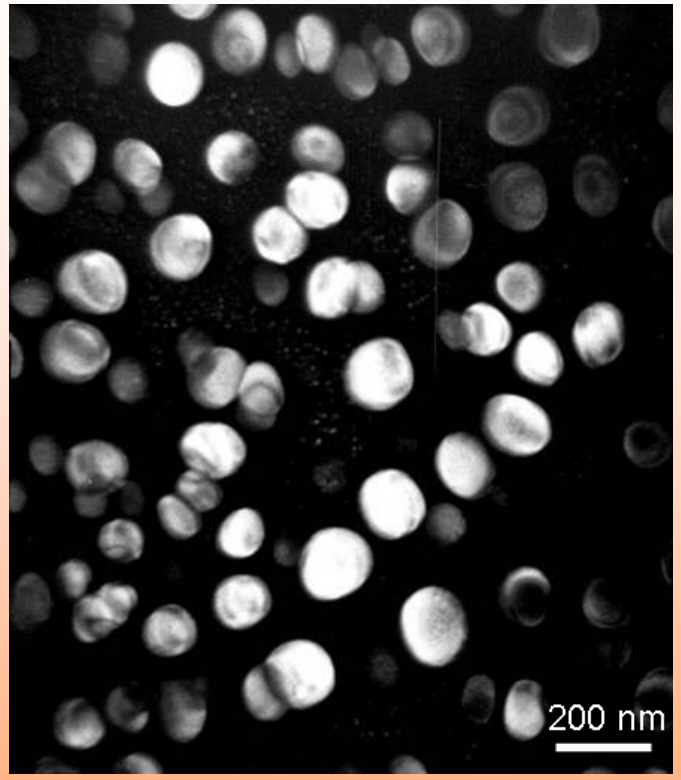

Air-cooled

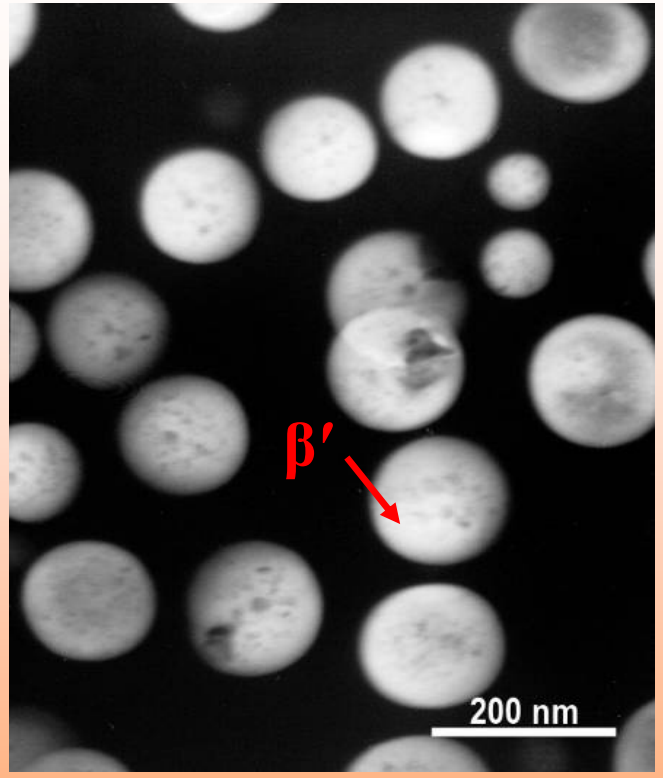

Annealed at 973 K for 100 h

Fine NiAl-type precipitates are coherent with the matrix.

Precipitate-Size Data

Alloy No.	Air-Cooled (nm)	973 K/100 hours (nm)	V_{973}/V_{AC}
FBB-1 (Base)*	15 ± 3.1	95.7 ± 20.5	260
FBB-2 (0.25Hf)	24.4 ± 4.5	91.8 ± 31	53
FBB-3 (0.25Zr)	22.8 ± 3.5	93.3 ± 22.1	69

***FBB-1: Fe-10Al-10Ni-10Cr**

The ratio of the mean volumes of precipitates, V_{973}/V_{AC} [$=(D_{973}/D_{AC})^3$] , as a relative measure of coarsening resistance. Zr is as good as Hf, as far as imparting coarsening resistance.

Effects of Al wt.% on the RT Ductility

Bending strain can be calculated by

$$\epsilon_f = \frac{6Dd}{L^2}$$

Where ε_f = bending strain, D = maximum deflection of the center of the beam, d = thickness, and L = support span

Alloys No.	Bending Strain (%)
FBB-1 (Based)	0.47
FBB-3 (10Al)	0.50
FBB-7 (8Al)	0.45
FBB-8 (6.5Al)	0.94
FBB-12 (4.0Al)	1.47

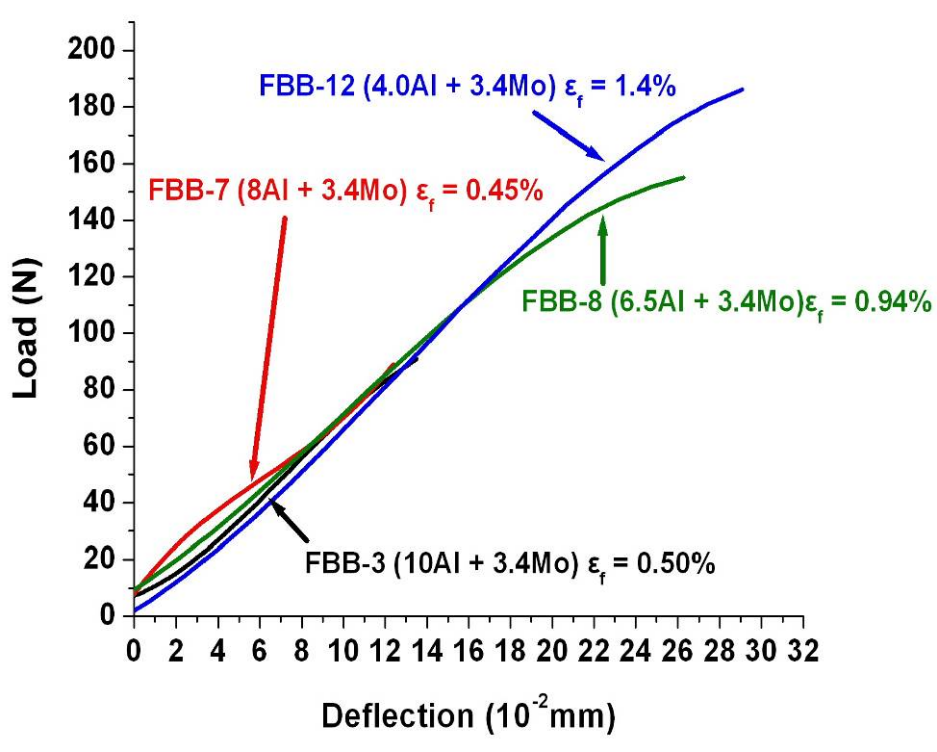

Load-deflection curves of alloys with different Al%

Reducing the Al% results in increased ductility.

Effects of Hot Forging on the RT Ductility

- Experimental:

Size = 12.7 mm × 12.7 mm × 4 mm

40% deformation at 1,173K

↓

Recrystallized at 1,173K for 1 hour

↓

Another 40% deformation at 1,173K

Alloys No.	Bending Strain (%) (Before Forging)
FBB-8 (6.5Al + 3.4Mo)	1.17 (0.94)
FBB-12 (4.0Al + 3.4Mo)	5.02 (1.47)

Hot forging can improve the ductility at room temperature, but its beneficial effect varies with alloy composition

Effects of Al wt.% on the Creep Property

Constant compressive stress of 140 MPa at 973K for 100 hours in air

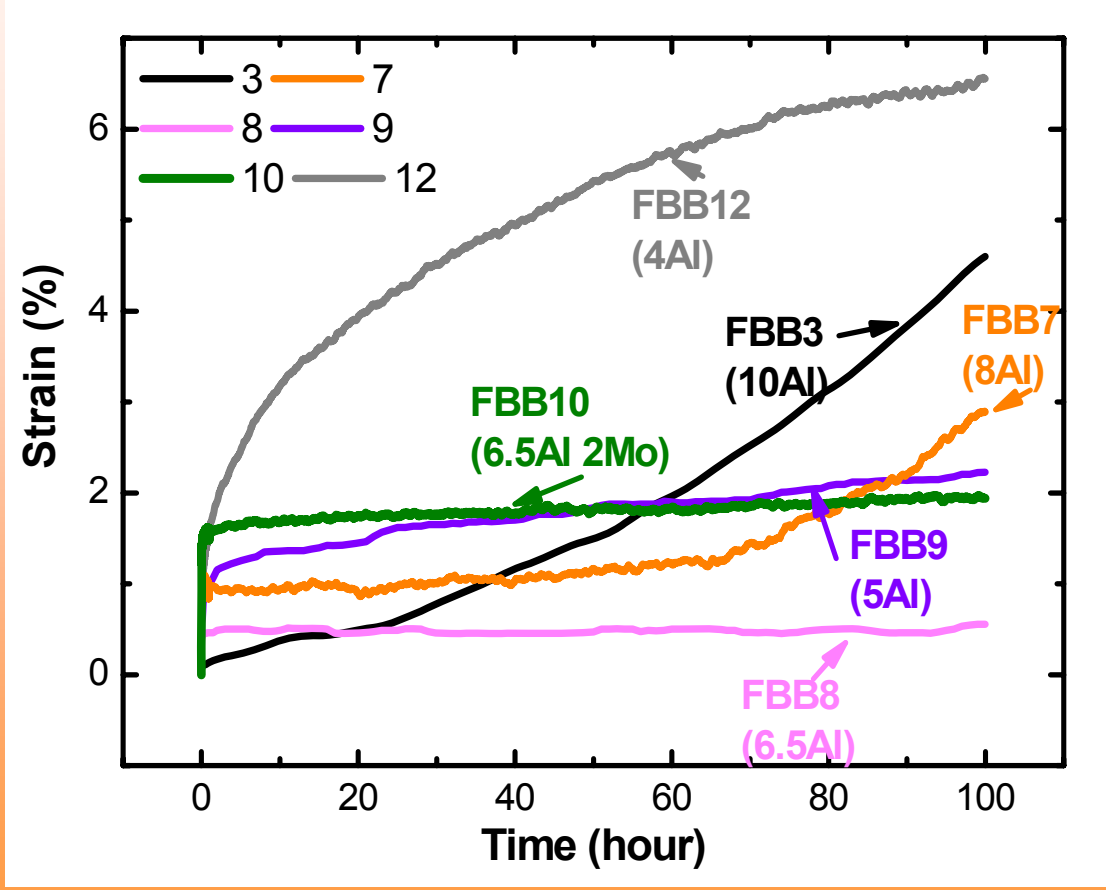

Alloys No.	Creep Rate (/s)
FBB3 (10Al)	8.0×10^{-8}
FBB7 (8.0Al)	4.7×10^{-8}
FBB8 (6.5Al)	~ 0
FBB9 (5.0Al)	2.6×10^{-8}
FBB10 (6.5Al+2Mo)	7.5×10^{-9}
FBB12 (4.0Al)	9.8×10^{-8}

The optimal Al concentration is around 5 ~ 6.5 wt.%.

Excellent Creep Resistance of FBB Alloys

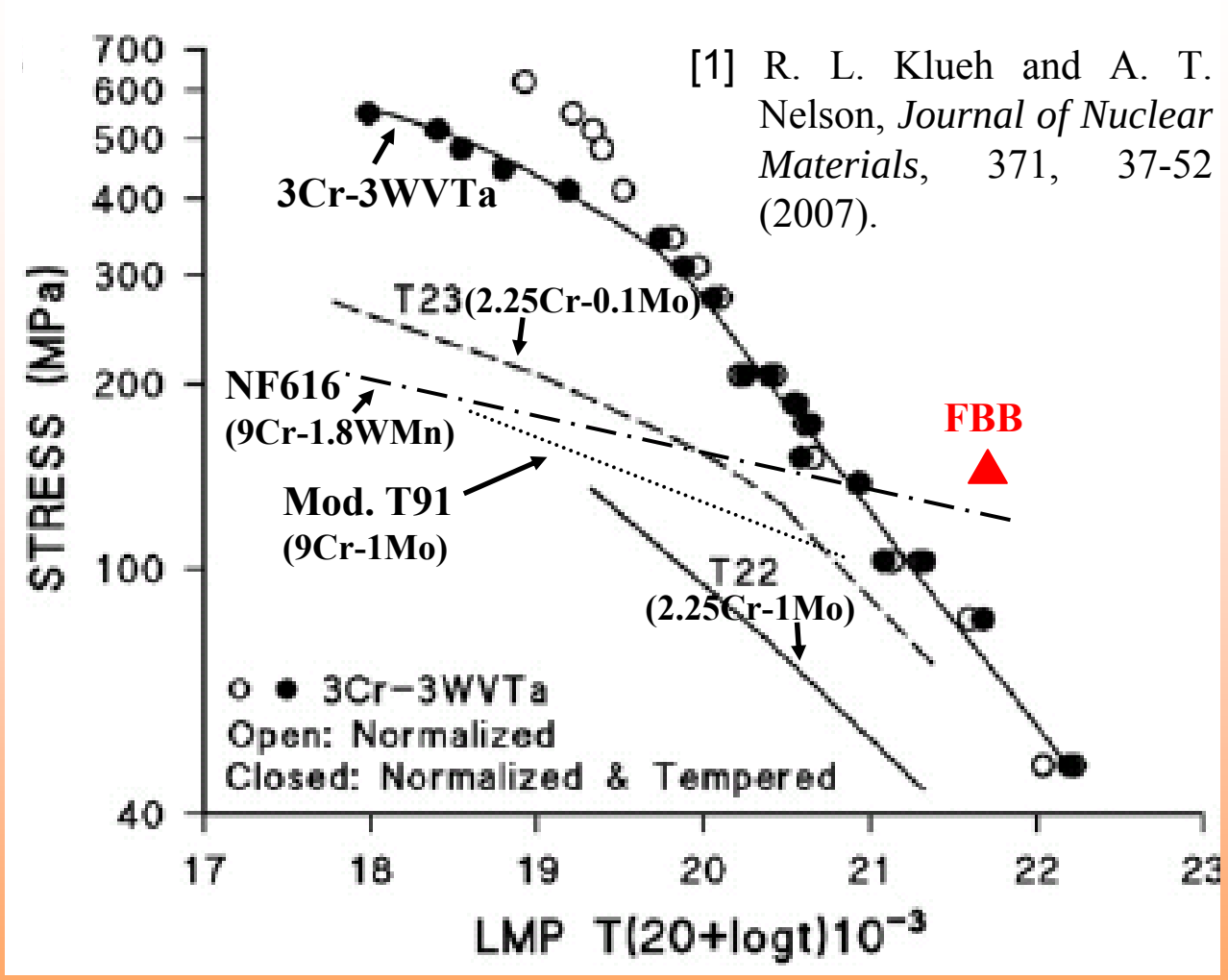

- Assume 10% rupture strain with a creep rate 1×10^{-8}/s at 140 MPa and 973K
- Compare with heat-resistant high and low Cr ferritic steels

Larson-Miller Parameter (LMP) of FBB:
t_r = 2,778 h $T(20 + \log t_r)$ = 21,800

Computer-aided Alloy Design

- **Understand diffusion characteristics and coarsening mechanisms**

- **Optimize alloy compositions for creep resistance**

-- Perform first-principles calculations of diffusivity

Experimental Diffusivity Results

Compilation of Published Data at T = 1,050K

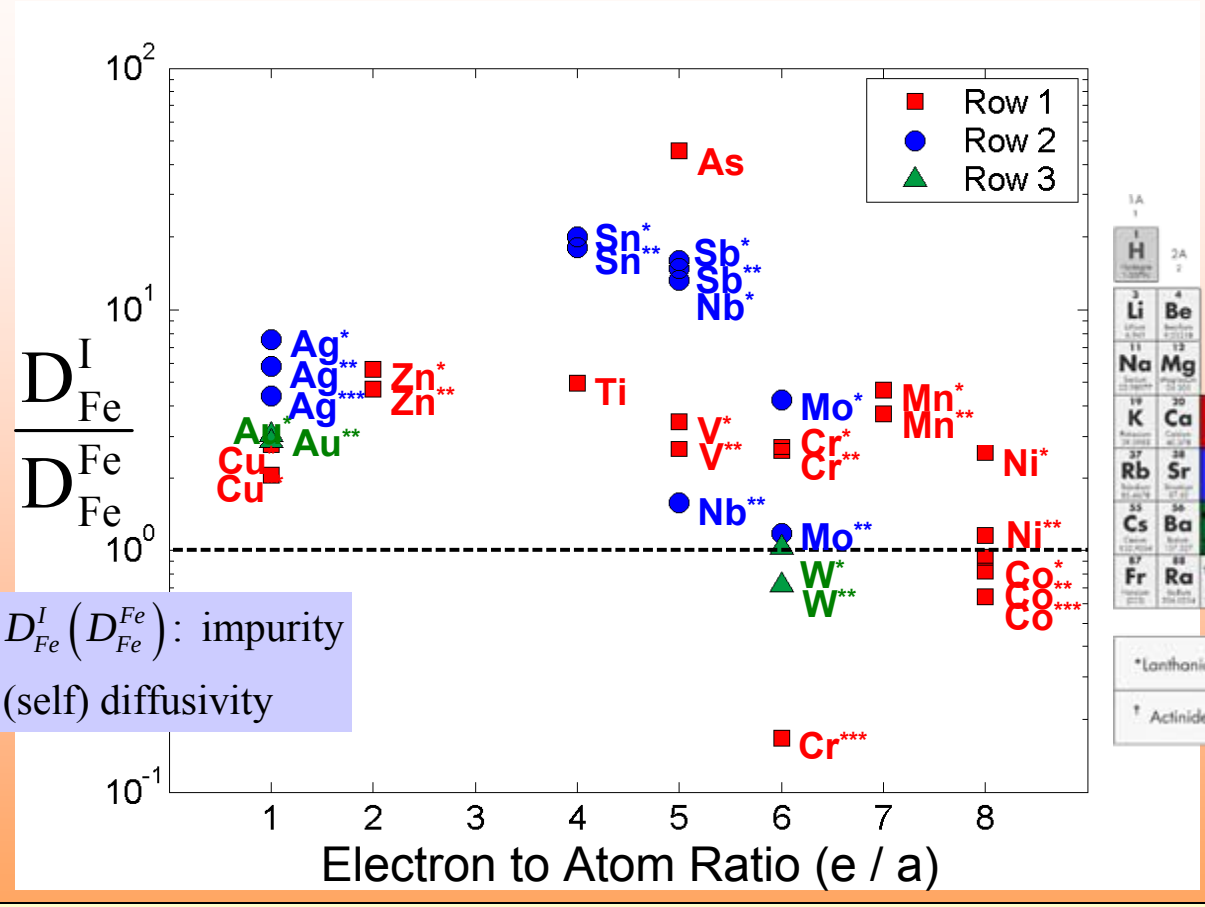

$D^I_{Fe}\left(D^{Fe}_{Fe}\right)$: impurity (self) diffusivity

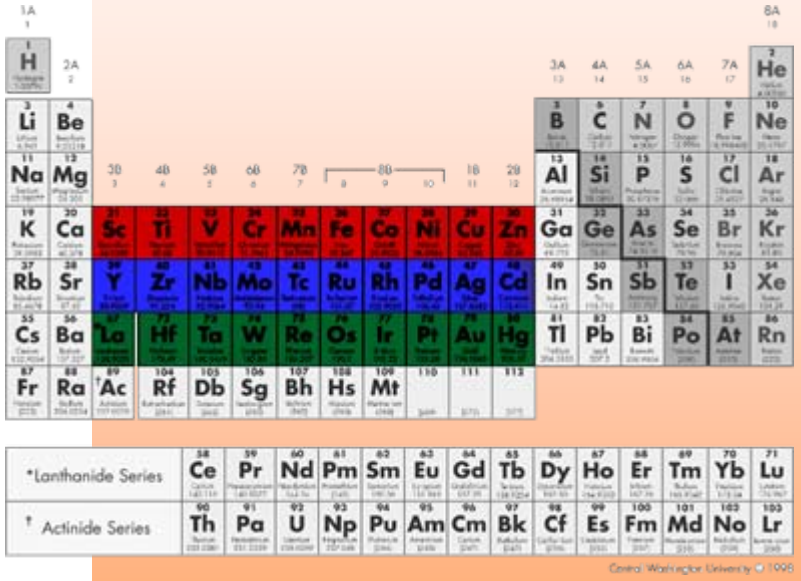

- Wide Scatter in Published Data for Several Solutes
- Data Lacking for Most 5d Solutes (Impurities)
- Absence of Clear Slow Diffusers in Measured Data

Model for Diffusivities

$$D_A^B = D_{0A}^{\ B} \exp[-Q_A^B / k_B T]$$

$D_A^B \left(D_A^A\right)$: impurity(self) diffusivity
D_0: diffusion prefactor
Q: activation energy
k_B: Boltzmann constant
T: temperature

Self Diffusion in α -Fe

$$D_{0Fe}^{\ Fe} = \frac{k_B T}{h} a^2 f_{bcc} \exp\left[\frac{\Delta S_v^f + \Delta S_v^{mig,Fe}}{k_B}\right]$$

$$Q_{Fe}^{Fe} = \Delta H_v^f + \Delta H_v^{mig,Fe}$$

Impurity Diffusion

$$D_{0Fe}^{\ I} = \frac{k_B T}{h} a^2 f_{Fe}^I \exp\left[\frac{\Delta S_v^f + \Delta S_v^{bind} + \Delta S_v^{mig,I}}{k_B}\right]$$

$$Q_{Fe}^I = \Delta H_v^f + \Delta H_v^{bind} + \Delta H_v^{mig,I}$$

a: lattice constant of matrix
h: Planck constant
f: correlation factor
ΔS_v^f: vacancy formation entropy
ΔS_v^{mig}: vacancy migration entropy
ΔS_v^{bind}: vacancy-solute binding entropy
ΔH_v^f: vacancy formation energy
ΔH_v^{bind}: vacancy-solute binding energy
ΔH_v^{mig}: vacancy migration energy

Diffusivity Calculations Require Methods for Computing:

- Vacancy Formation, Binding, and Migration Energies
- Vacancy Formation, Binding, and Migration Entropies
- Correlation Factors for Impurity Diffusion

First-Principles Calculations

- Vacancy Formation, Migration, and Binding Energies
  - VASP, Projector-Augmented Wave (PAW), Spin-Polarized Generalized Gradient Approximation (GGA)
  - 128-Atom Supercells
- Entropies
  - Harmonic vibrational contributions
    - Direct force-constant approach using 54-atom supercells
  - Electronic contributions included
- Saddle-Point Geometry
  - Mid-Point between Vacancy and Solute Neighbors Assumed
  - Verified by Nudged-Elastic Band for W, Fe, and Hf

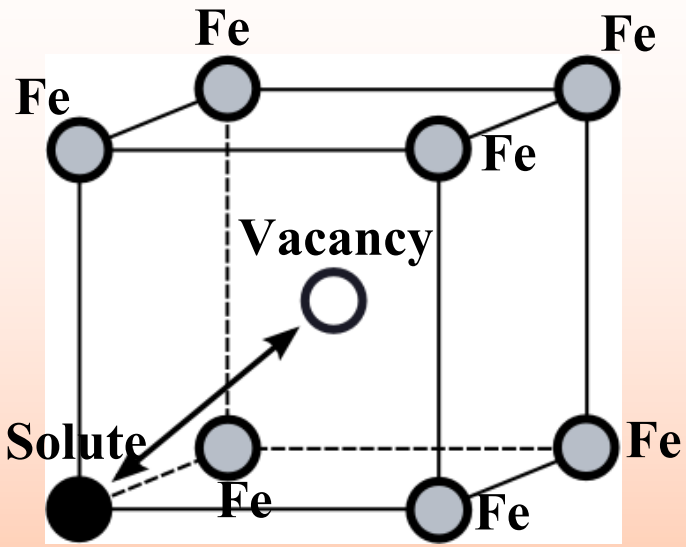

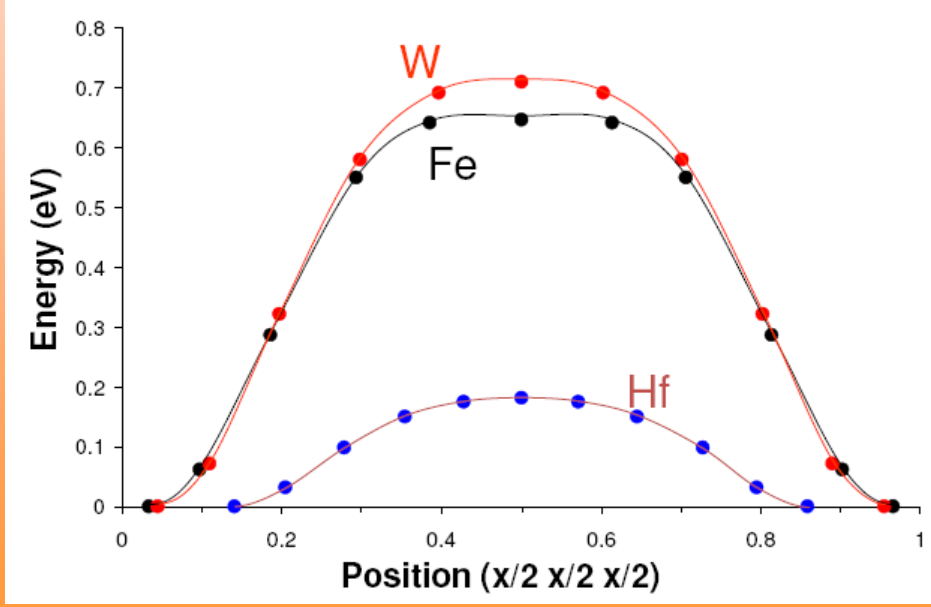

Activation Energies: Magnetic Contributions

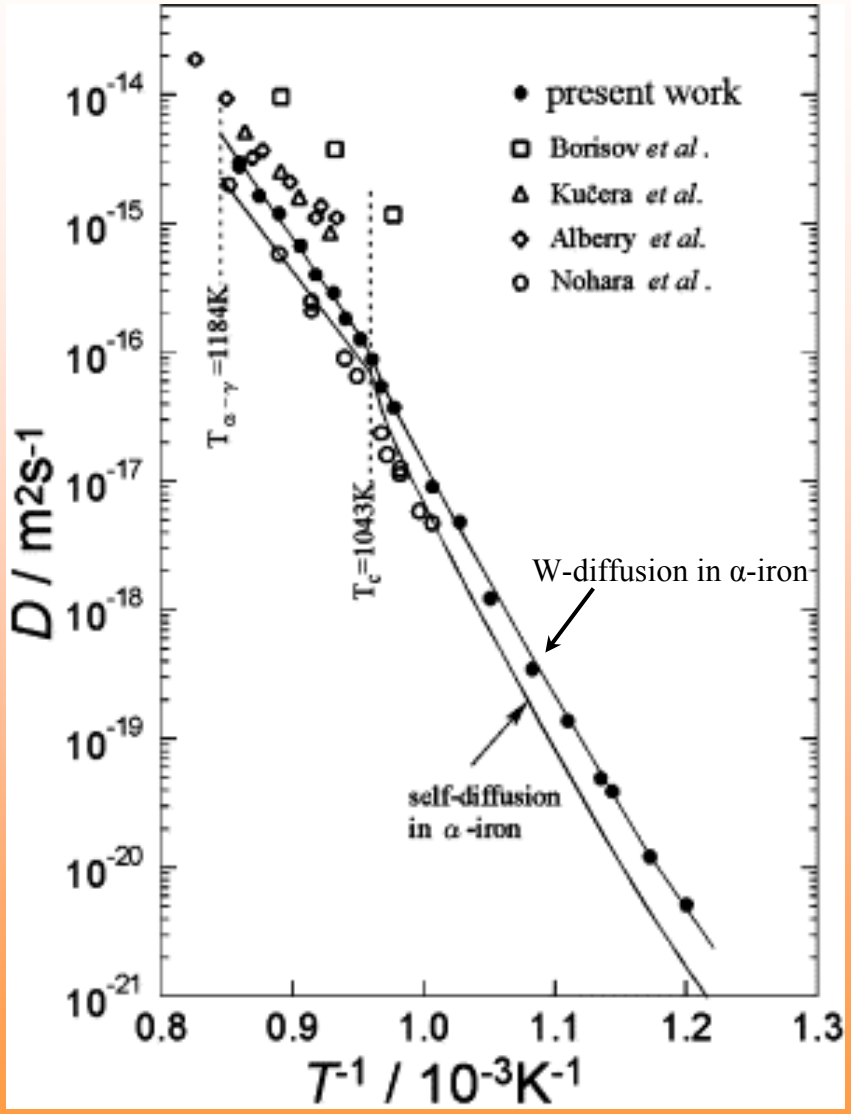

S. Takemoto, H. Nitta, Y. Iijima, and Y. Yamazaki, *Phil Mag., 2007*, v. 87, p 1619.

- Magnetic Contribution in Ferromagnetic Phase: α

$$Q^F(T) = Q^P\left[1 + s(T)^2\alpha\right]$$
$$s(T) = M(T)/M(0)$$

Q^F, Q^P : diffusion activation energy in a ferromagnetic, paramagnetic state

$s(T)$: a ratio of the magnetization, M, at T and zero temperature

- α quantifies influence of magnetic ordering on activation energy, Q
- α measured for relatively few solutes (impurities)

Semi-Empirical Model for α

- Linear Empirical Relation: α and Induced Magnetization

$$\alpha \propto \Delta M_{12}$$

$$\Delta M_{12} = \sum_{i=1}^{8} \Delta m_i^{1st\ NN} + \sum_{j=1}^{6} \Delta m_j^{2nd\ NN}$$

S. Takemoto, H. Nitta, Y. Iijima, and Y. Yamazaki, *Phil Mag., 2007*, v. 87, p. 1619.

ΔM_{12}: the induced magnetization of the impurity in the first and second neighbors

- Calculate ΔM_{12} for solutes with known α
- Develop a linear relationship:

$$\alpha = 0.0586\Delta M_{12} + 0.1591$$

- Predict α for other solutes

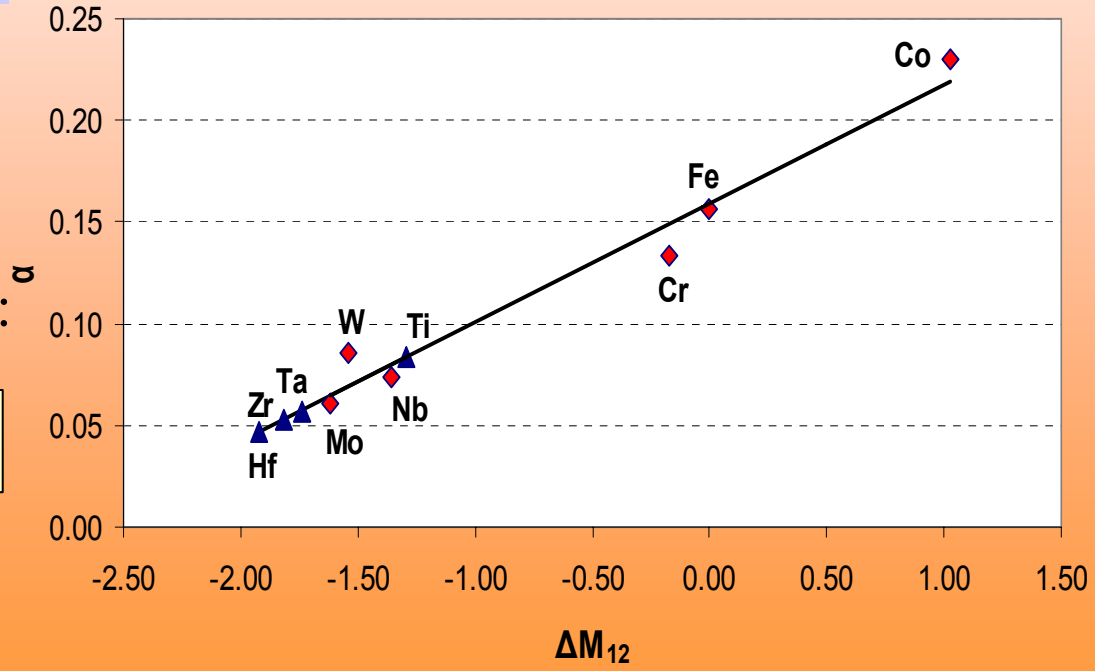

Validation of Computational Approach

Fe Self Diffusion

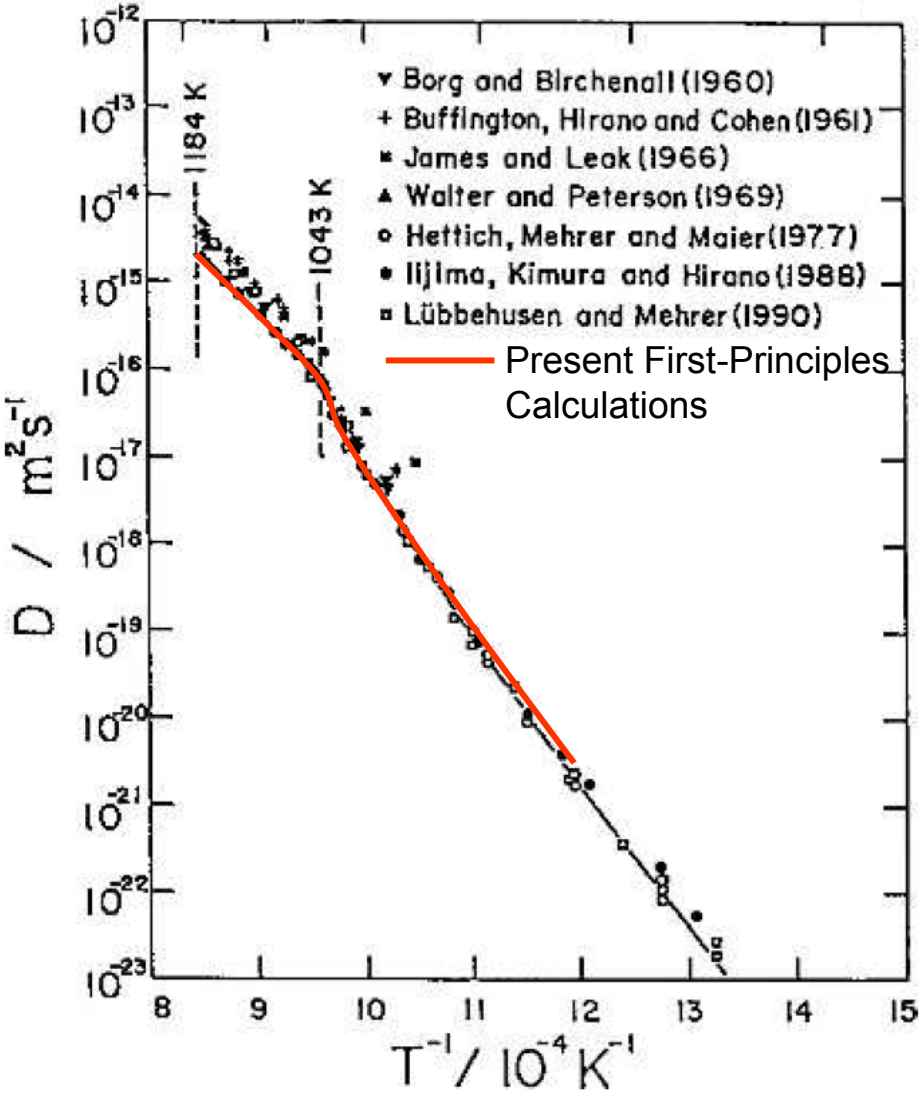

W Impurity Diffusion

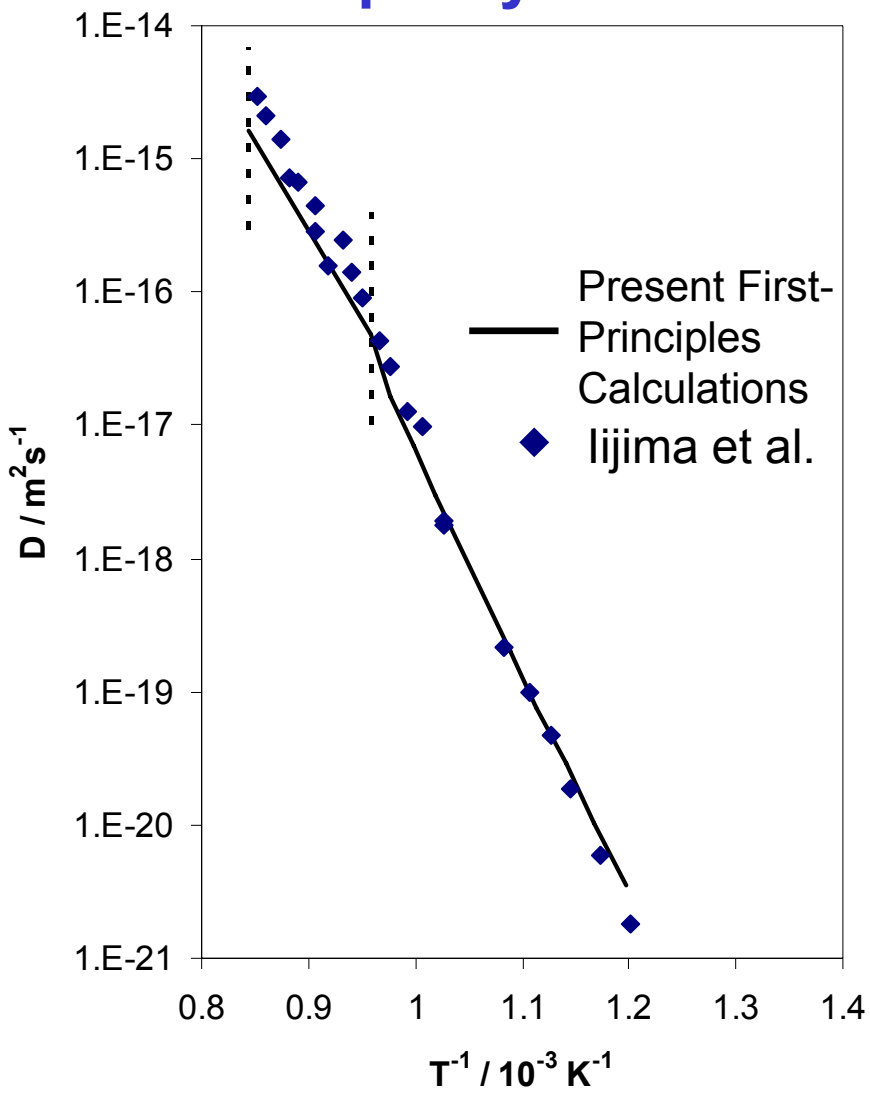

First-Principles Results for Other Solutes

Solute	$\Delta H_v^{mig,I}$ kJ / mol	ΔH_v^{bind} kJ / mol	$Q^{F\,I}_{Fe}$ kJ / mol
Fe	**62.2**	**0**	**277.1**
W	**68.3**	**-13.1**	**283.2**
Mo	**51.8**	**-16.2**	**266.7**
Zr	**4.3**	**-78.4**	**219.2**
Ta	**42.4**	**-30.9**	**257.3**
Hf	**17.1**	**-62.9**	**232.0**
Ti	**31.1**	**-25.3**	**245.9**

Conclusions

- Prototype Fe-based alloys containing β and β' phases exhibit microstructures analogous to the classical Ni-based γ/γ' superalloys.

- The reduction of Al concentration and the introduction of hot forging are both effective to improve the ductility of FBB alloys at room temperature.

- The optimal creep resistance can be obtained while the Al concentration is about 6 wt.%.

Conclusions (Cont'd)

- Methods for calculating impurity diffusion coefficients in α-Fe based on 1st-principles calculations
  - Calculations of vacancy formation, migration, and binding energies and entropies
  - Semi-empirical correction for magnetic disorder
- Comparison with Experimental Data
  - Results of calculations comparing favorably for Fe self diffusion and W impurity diffusion
- Calculated activation energies for selected 4d and 5d solutes
  - General trend towards strong vacancy binding
  - Except for W, migration energies lower relative to pure Fe
- Search for very slow diffusers continues…

Scientific Basis for Microstructural Design

γ/γ′phases in a Ni-based alloy (Ni-22Cr-15Fe) (wt.%) [1]

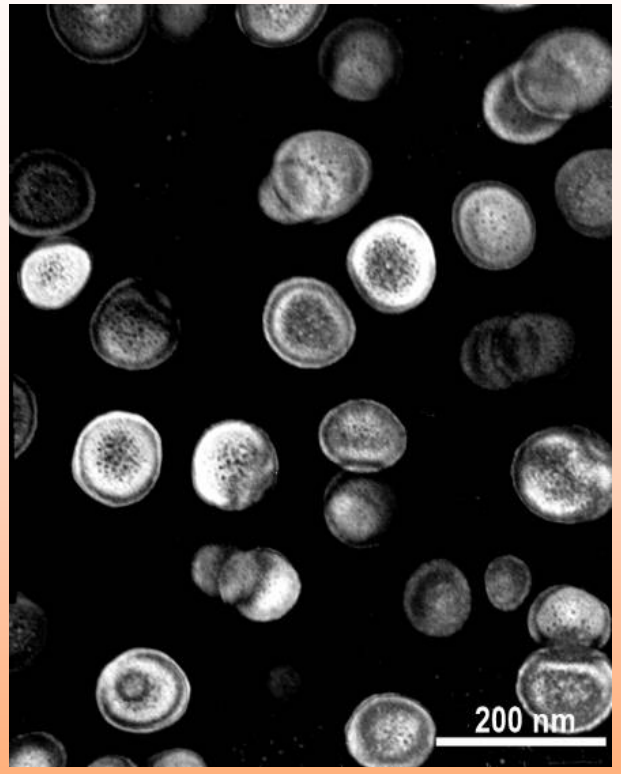

β/ β′ phases in an Fe-based alloy (Fe-8Al-10Ni-10Cr) (wt.%), present work

Nickel-based γ/γ′ superalloys owe their excellent creep strength to the presence of a high volume fraction of coherent-coplanar ordered γ′ precipitates.

Like γ/γ′ systems, the body-centered cubic (bcc) Fe-matrix (A2 or β) and NiAl-type (B2 or β′) precipitates exhibit cube-on-cube or coplanar orientation relationship.

[1] Neal D. Evans, Philip J. Maziasz, and John J. Truhan, “Phase Transformation During Service Aging of Nickel Based Superalloy Pyromet 31V”.

Wet-Chemical Analyses

Concentration of the alloying elements in FBB alloys (wt.%)

Alloys #	Fe	Al	Ni	Cr	B	Mo	Zr	Hf
FBB-2	66.53	9.84	9.97	9.88	0.005	3.37	-	0.25
Designed goal	66.3	10	10	10	0.005	3.4	-	0.25
FBB-3	66.57	9.81	10.05	9.88	0.005	3.37	0.25	-
Designed goal	66.3	10	10	10	0.005	3.4	0.25	-

FBB alloys were successfully fabricated by arc-melting and drop into the Cu mode with a dimension of 12.7 mm × 12.7 mm × 76.2 mm

Fracture Surfaces of Bend-Tested Alloys: Brittle Cleavage

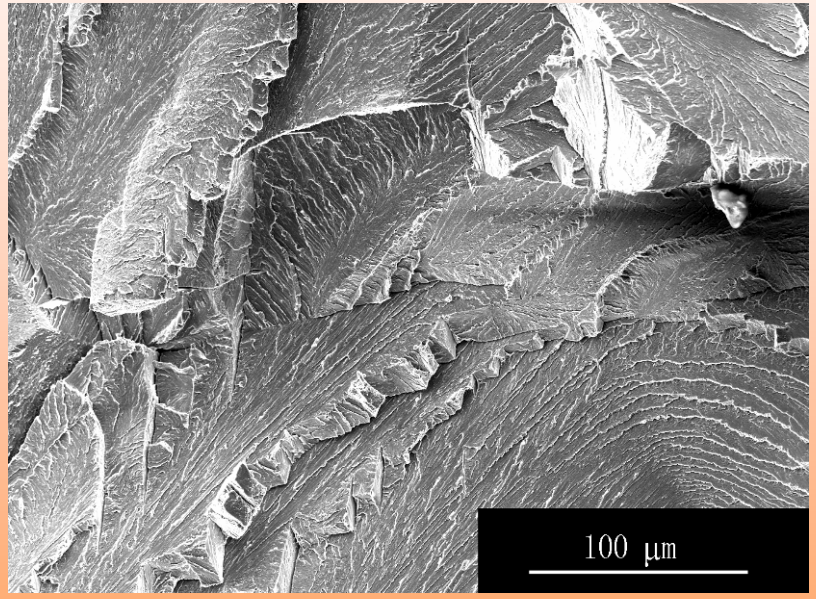

FBB-5 containing 10 wt.% Al

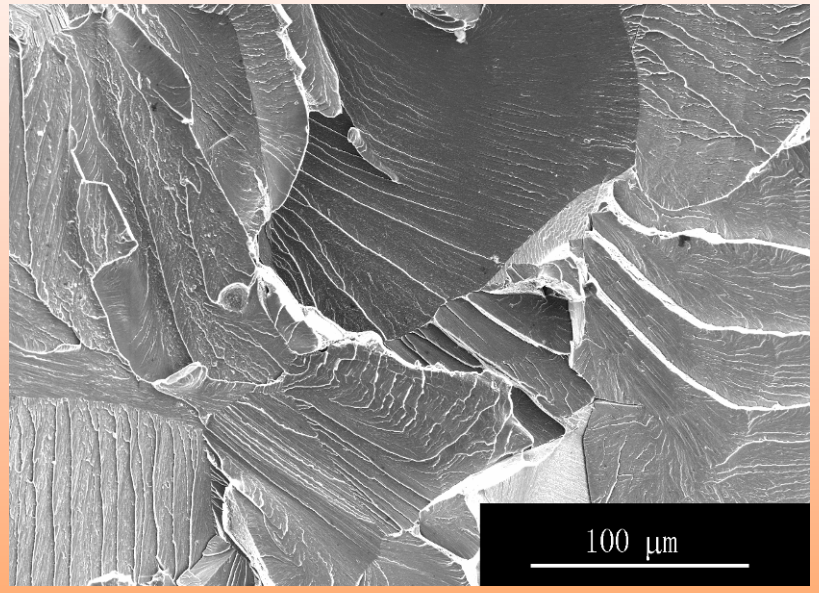

FBB-8 containing 6.5 wt.% Al

Correlation Factors

- Correlation factors calculations
  - Generalization of Manning's 5-frequency model using a transition-matrix approach [1]
  - Frequencies from first-principles calculated activation energies
- Correlation factor ratio found to be ~ 1 for solutes at all temperatures.

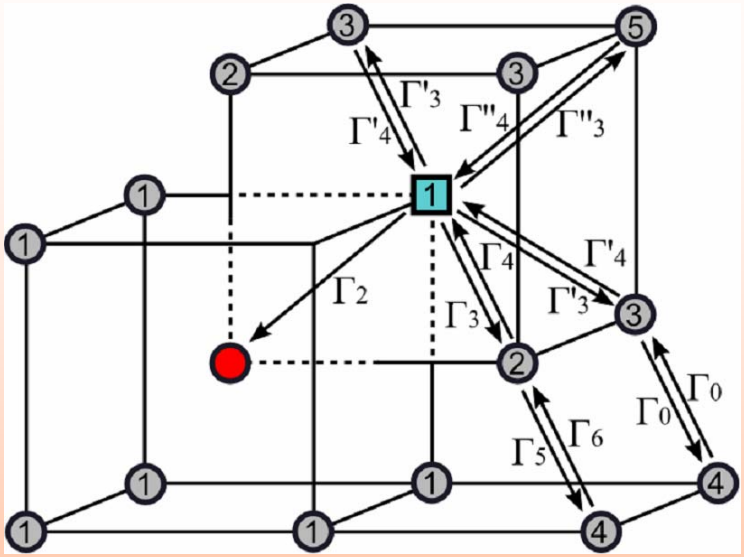

Impurity Atom

Vacancy

Solute	f_A^B / f_A^A @ 1,050K
W	1.050
Mo	1.109
Zr	0.975
Hf	0.896

$$f = \frac{1 + \langle \cos(\theta) \rangle}{1 - \langle \cos(\theta) \rangle}$$

$\langle \cos(\theta) \rangle$: average cosine angle between successive jumps of the impurity

[1] J. R. Manning. *Diffusion Kinetics For Atoms in Crystals*, 1968.

Excellent Creep Resistance of FBB Alloys

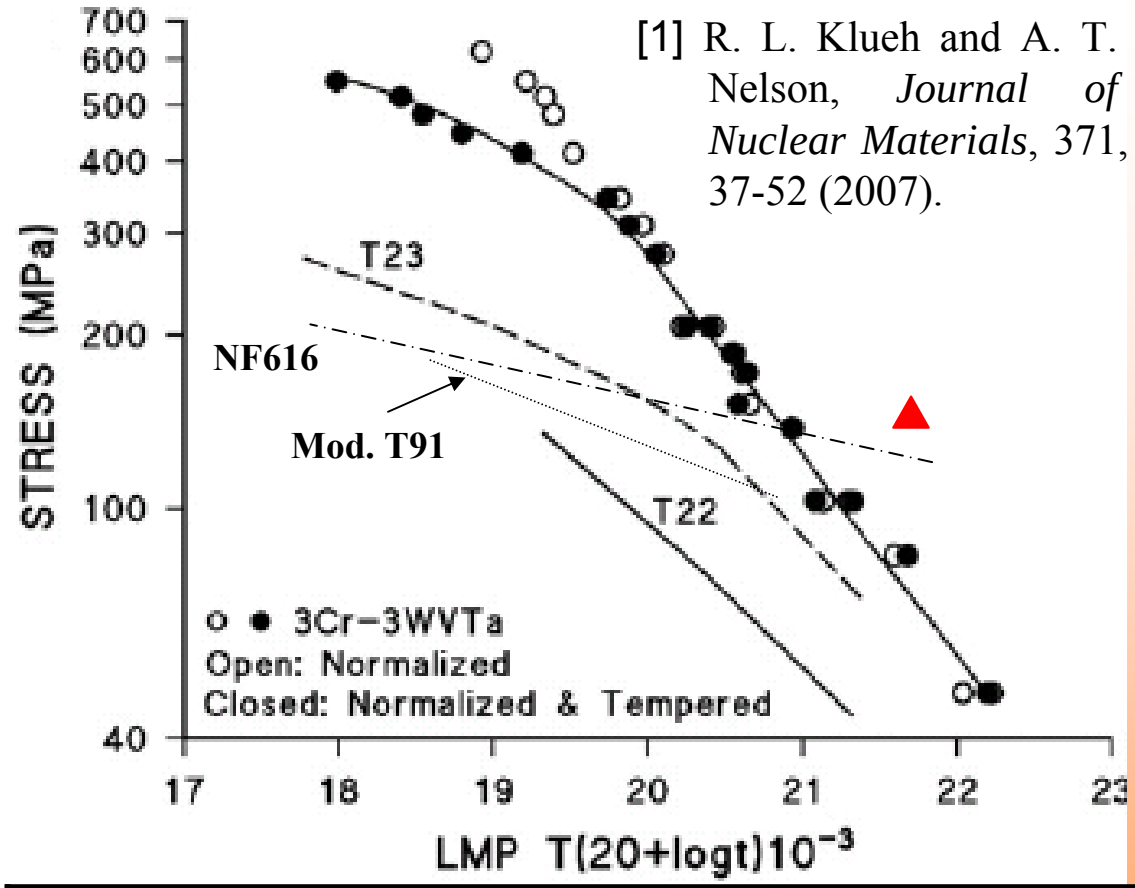

- Assume 10% rupture strain with a creep rate 1×10^{-8}/s at 140 MPa and 973K
- Compare with heat-resistant high and low Cr ferritic steels

Larson-Miller Parameter (LMP) of FBB:
t_r = 2778 h
$T(20 + \ln t_r) = 21{,}800$
Highest!

steel	C	Si	Mn	Cr	Ni	Mo	W	V	Nb	B	N	Ta
T22	0.15	0.3	0.45	2.25	-	1.0	-	-	-	-	-	-
T23	0.06	0.2	0.45	2.25	-	0.1	-	0.25	0.06	0.003	-	-
NF616	0.07	0.06	0.45	9.0	0.25	0.5	1.8	0.2	0.05	0.004	0.06	-
Mod. T91	0.1	0.4	0.4	9.0	0.1	1.0	-	0.2	0.08	-	0.05	-
3Cr-3WVTa	0.1	0.14	0.5	3.0	-	-	3.0	0.25	-	-	-	0.1